Heat and Mass Transfer of a Chemically Reacting MHD Micropolar Fluid Flow over an Exponentially Stretching Sheet with Slip Effects

E. O. Fatunmbi[1*] and O. J. Fenuga[2]

[1]*Department of Mathematics and Statistics, Federal Polytechnic, Ilaro, Nigeria.*
[2]*Department of Mathematics, University of Lagos, Nigeria.*

Authors' contributions

This work was carried out in collaboration between both authors. Author EOF formulated the problem of the study, solved the derived differential equations governing the fluid flow and wrote the introduction. Author OJF discussed the results and carried out the analysis. Both authors read and approved the final manuscript.

Original Research Article

ABSTRACT

This work investigates flow, heat and mass transfer of a chemically reacting and electrically conducting micropolar fluid over an exponentially stretching sheet in the presence of thermal radiation, viscous dissipation, suction/injection, heat source/sink and slip effects. The system of the governing partial differential equations of the fluid flow is transformed into nonlinear ordinary differential equations by applying similarity variables. The resulting equations are numerically solved via shooting method alongside fourth order Runge-Kutta integration technique. The influences of the controlling flow parameters on the dimensionless velocity, angular velocity, temperature and species concentration profiles as well as on the skin friction coefficient, wall couple stress coefficient, heat and mass transfer rates are presented through graphs and tables. Comparison of the present results with previously published work in the literature for some limiting cases shows a good agreement.

Keywords: Micropolar fluid; exponential stretching; slip effects; suction/injection.

---

*Corresponding author: E-mail: olusojiephesus@yahoo.com, olusojiephesus_1@yahoo.com, fatunmbi@federalpolyilaro.edu.ng

NOMENCLATURES

x and y : cartesian coordinates [m]
u and v : velocity component along x, y respectively [ms^{-1}]
N : microrotation component perpendicular to x-y plane [s^{-1}]
L : characteristics length [m]
T : fluid temperature inside the boundary layer [K]
C : species concentration of the fluid inside the boundary layer [$molm^-3$]
C_w : species concentration at wall/plate [$molm^-3$]
C_∞ : free stream species concentration [$molm^-3$]
T_w : fluid temperature at wall [K] T_∞: free stream temperature [K]
u_w, u_∞ : velocity of the stretching sheet, free stream velocity [ms^{-1}]
Q_0 : heat generation coefficient [$Wm^{-3}K^{-1}$]
k_r : constant rate of chemical reaction [Mol/s]
V_w : suction/injection velocity [ms^{-1}]
k : thermal conductivity coefficient [$Wm^{-1}K^{-1}$]
B_0 : magnetic field strength [A/m]
j : micro-inertia per unit mass [kgm^{-3}]
q_r : radiative heat flux [Wm^{-2}]
Cp : specific heat at constant pressure [J/kgK]
$f(\eta)$: dimensionless stream function

GREEK SYMBOLS

P : density of the fluid [kgm^{-3}]
Ψ : stream function [m^2s^{-1}]
Σ : electric conductivity [Sm^{-1}]
N : kinematic viscosity [m^2s^{-1}]
μ : dynamic viscosity [$kgm^{-1}s^{-1}$]
γ : spin gradient viscosity [m^2s^{-1}]
$\sigma^\star$: Stefan-Boltzmann constant [$Wm^{-2}K^4$]
$\alpha^\star$: mean absorption coefficient [m^{-1}]
η : dimensionless scaling transformation variable
$\theta(\eta)$: dimensionless temperature
$\varphi(\eta)$: dimensionless species concentration
λ : microrotation density parameter
ζ : reaction rate parameter

1. INTRODUCTION

In the recent times, engineers and researchers have developed interest in the study of non-Newtonian fluids due to the increasing practical usefulness and relevance of these fluids in many industrial and technological processes like polymer engineering, crude oil extraction, food processing manufacturing and many others. Among the various non-Newtonian fluids models, the micropolar fluids theory developed by Eringen [1] and extended to thermo-micropolar fluids also by Eringen [2] has gained prominence. This is because the theory of micropolar fluids provides a good mathematical model for investigating the flow of complex and complicated fluids such as suspension solution, animal blood, liquid crystals, polymeric fluids and clouds with dust [3-4].

Micropolar fluids are fluids with microstructure which belong to the class of fluids that exhibit certain microscopic effect arising from the local structure and micromotion of the fluid element. Physically, micropolar fluids may represent fluids consisting of rigid, randomly oriented (or spherical) particles suspended in a viscous medium, where particles deformation is ignored, they also belong to the group of fluids with non-symmetric stress tensor that are called polar fluids which constitute a substantial generalization of the Navier-Stokes model. Such fluids are of a complex nature and individual fluid particles may be of different shapes and may

shrink and/or expand, occasionally changing shapes and rotating independently of the rotational movement of the fluid Lukaszewicz [5]. Peddieson and McNitt [6] first studied the boundary layer flow of such fluids, thereafter, several authors have investigated these fluids on different geometries and conditions.

The boundary layer flow past stretching sheet is significant in engineering and industrial processes such as extrusion of plastic sheet, glass blowing, continuous casting and spinning of fibers, hot rolling, textile and paper production. Specifically, various metallurgical operations have to do with the cooling of continuous strips or filaments by drawing them in a quiescent fluid and in the process of drawing, the strips are sometimes stretched. The quality of the final product depends to some extent on the kinematic of stretching and the rate of cooling. In such cases, the rate of cooling can be controlled by drawing such strips in an electrically conducting fluid subjected to a magnetic fluid such that the end product can be obtained with desired characteristics. Pioneering the work on boundary layer flow induced by stretching sheet, Crane [7] investigated linearly stretching sheet on the steady two-dimensional problem and gave the similarity solution in closed analytical form, Gupta and Gupta [8] extended the work of Crane to include heat and mass transfer on stretching sheet with suction or blowing. Eldabe et al. [9] studied MHD flow of a micropolar fluid past a stretching sheet with heat transfer. Elbashbeshy and Bazid [10] examined heat transfer over a stretching sheet embedded in a porous medium. Recently, Reddy [11] examined heat generation and thermal radiation effects over a stretching sheet in a micropolar fluid.

In some practical situations, however, the stretching of plastic sheet may not necessarily be linear, it may be nonlinear and/or the exponential type. The flow, heat and mass transfer characteristics over an exponentially stretching sheet has numerous applications in technology such as in the case of annealing and thinning of copper wire. In such cases, the end product depends on the rate of heat transfer at the stretching continuous surface with exponential variations of stretching velocity and temperature distribution (Mukhopadhyay [12]). However, a little attention has been paid to the study of flow over an exponentially stretching sheet in spite of its important applications in many engineering operations. Pioneering the work on flow over an exponentially stretching sheet, Magyari and

Keller [13] studied heat and mass transfer on boundary layer flow induced an exponentially stretching sheet with exponential temperature distribution. Later, Sajid and Hayat [14] considered the influence of thermal radiation on the boundary layer flow due to exponentially stretching sheet. El-Aziz [15] extended the work of Magyari and Keller [13] by investigating viscous dissipation effect on mixed convection flow of a micropolar fluid over an exponentially stretching sheet. Mandal and Mukhopadhyay [16] investigated heat transfer analysis for fluid flow over an exponentially stretching porous sheet with surface heat flux. Recently, Seini and Makinde [17] examined MHD boundary layer flow of a Newtonian fluid due to exponentially stretching surface with radiation and chemical reaction.

Magnetohydrodynamic (MHD) is the interaction between moving electrically conducting fluid and magnetic field. The applications of magnetic field in engineering problems are enormous, these include plasma studies, nuclear reactors, oil exploration, geothermal energy extractions, MHD generators, and boundary layer control in the field of aerodynamic. To this end, several authors have studied MHD boundary layer flow, Daniel [18] investigated steady MHD boundary-layer slip flow and heat transfer of Nanofluid over a convectively heated of non-linear permeable sheet. Kumar [19] numerically studied the problem of heat and mass transfer in a hydromagnetic flow of a micropolar fluid past a stretching sheet using the Finite element technique. It was reported that the fluid velocity increased with a rise in the material parameter while the opposite was the case with increase in the magnetic field parameter. Similarly, microrotation, concentration and temperature profiles increased as the magnitude of the magnetic field parameter increased.

Many of the engineering and manufacturing operations occur at high temperature, the effect of radiative transfer on magnetohydrodynamic flow, heat and mass becomes practically important for the design of relevant equipment, steel rolling, nuclear power plants, electric power generation, hypersonic flights, space vehicles, gas turbines. Due to these applications, many researchers have reported the influence of thermal radiation on fluid flow. Daniel et al. [20] studied the impact of thermal radiation on electrical MHD flow of nanofluid over nonlinear stretching sheet with variable thickness. Also, the influence of thermal radiation on unsteady

electrical MHD flow of nanofluid over stretching sheet with chemical reaction has been carried out by Daniel et al. [21]. Biswas et al. [22] studied the effects of radiation and chemical reaction on MHD unsteady heat and mass transfer of Casson fluid flow over a vertical plate. Daniel and Daniel [23] analytically examined the effects of buoyancy and thermal radiation on MHD flow over a stretching porous sheet by the application of homotopy analysis. The authors pointed out that a rise in the thermal radiation parameter causes significant increase in the thermal conditions of the fluid as well as increase in the hydrodynamic boundary layer and thermal boundary layer thicknesses.

The study of boundary layer flow involving chemical reaction andheat generation/absorption has drawn the attention of many researchers due to its important applications in many engineering processes such as in chemical processes and hydrometallurgical industries, for example, food processing, smog formation, groves of fruit trees and crop damage due to freezing and manufacturing of ceramics and polymer production (Das [24]; Mishra et al. [25]). Likewise, heat generation/absorption effect may change the temperature distribution of the fluid flow and in consequence affect various engineering devices. Such study has attracted researchers such as (Ibrahim, [26]; (Olajuwon et al. [27]; Fatunmbi and Odesola [28]; Pal and Chatterjee [29]).

Many of the researchers above have investigated the flow and heat transfer problems of Newtonian/non-Newtonian fluids with the assumption of no-slip boundary condition which is the central tenets of the Navier-Stokes theory. However, it has been observed that the assumption of no-slip boundary condition does not hold in some practical situations and hence, it may be necessary to replace the no-slip boundary condition with the partial slip boundary conditions. The non-adherence of fluid to a solid boundary is known as velocity slip. The slip and temperature jump boundary conditions represent a discontinuity in the transport variable across the interface and describes more accurately the non-equilibrium region near the surface. Slip flow problems are important when considering particulate fluids e.g. emulsions, suspensions and polymer solutions in which there may be a slip between the fluid and the boundary (wang [30]). The applications of such study in technology can be found in the polishing of

artificial heart valves and internal cavities (Mukhopadhyay [12]). In view of this, Anderson [31] examined the slip-flow of a Newtonian fluid over a linearly stretching sheet, Daniel [32] investigated laminar convective boundary layer slip flow over a flat plate using Homotopy Analysis Method and pointed out that an increase in the slip parameter increases the velocity to a point that the hydrodynamic boundary layer becomes thinner. Das [24] investigated slip effects on heat and mass transfer in MHD micropolar fluid flow over an inclined plate with thermal radiation and chemical reaction. Devi et al. [33] examined radiation effect on MHD slip flow past a stretching sheet with variable viscosity and heat source/sink. Nandeppanavar et al. [34] investigated flow and heat transfer in MHD Newtonian fluid flow over a stretching sheet with variable thermal conductivity and partial slip.

Many of the reported investigations above have been done with Newtonian fluid however, complex mechanical behaviour that fluids exhibit at micro and nano scales, and the rheological characteristics of fluids of practical industrial importance can neither be captured nor explained by the Newtonian fluid mechanics (Chen et al. [3]). Hence, the aim of this study is to investigate the flow, heat and mass transfer in MHD non-Newtonian micropolar fluid under the influence of thermal radiation, higher order chemical reaction, viscous dissipation, heat generation/absorption, with velocity and thermal slips over an exponentially stretching sheet with exponential temperature and concentration distributions. The nonlinear partial differential equations of the flow are transformed into nonlinear ordinary differential equations by appropriate similarity transformations while the resulting equations are solved using the shooting technique with fourth order Runge-Kutta integration scheme.

2. PROBLEM FORMULATION

Consider a steady, two-dimensional, laminar boundary layer slip flow of a viscous, incompressible chemically reacting and electrically conducting micropolar fluid past an exponentially stretching sheet. The cartesian coordinate system is (x, y, z) and the corresponding velocity components are $(u, v, 0)$. The x axis is directed towards the continuous stretching sheet along the flow while the y axis is normal to it. The stretching velocity is assumed

to be $u_w = U_0 e^{\left(\frac{x}{L}\right)}$ while the velocity upstream is assumed to be zero. The temperature and concentration of the sheet are taken to be $T_w = T_\infty + T_0 e^{\left(\frac{x}{2L}\right)}$ and $C_w = C_\infty + C_0 e^{\left(\frac{x}{2L}\right)}$ respectively. The flow is confined to the region y > 0. A transverse variable magnetic field $B(x)$ is applied normal to the flow direction as displayed in Fig. 1. Also, the angular velocity is given as $\boldsymbol{N} = (0, 0, N(x, y))$ is assumed. The radiative heat flux term in x direction is considered negligible as compared to that in the y direction. It is assumed also that the magnetic Reynolds number is sufficiently small such that the induced magnetic field is negligible as compared to the applied magnetic field.

Under the stated assumptions and the boundary layer approximations, the governing boundary layer continuity, momentum, microrotation, energy and concentration equations are respectively given as:

$$\frac{\partial u}{\partial x} + \frac{\partial v}{\partial y} = 0 \tag{1}$$

$$u\frac{\partial u}{\partial x} + v\frac{\partial u}{\partial y} = \frac{(\mu + \kappa)}{\rho}\frac{\partial^2 u}{\partial y^2} + \frac{\kappa}{\rho}\frac{\partial N}{\partial y} - \frac{\sigma B^2(x)}{\rho}u \tag{2}$$

$$\rho j\left(u\frac{\partial N}{\partial x} + v\frac{\partial N}{\partial y}\right) = \gamma\frac{\partial^2 N}{\partial y^2} - \kappa\left(2N + \frac{\partial u}{\partial y}\right) \tag{3}$$

$$u\frac{\partial T}{\partial x} + v\frac{\partial T}{\partial y} = \frac{k}{\rho Cp}\frac{\partial^2 T}{\partial y^2} + \frac{(\mu + \kappa)}{\rho Cp}\left(\frac{\partial u}{\partial y}\right)^2 - \frac{1}{\rho Cp}\frac{\partial q_r}{\partial y}$$
$$+ \frac{\sigma B^2(x)}{\rho}u^2 + \frac{Q_0}{\rho C_p}(T - T_\infty) \tag{4}$$

$$u\frac{\partial C}{\partial x} + v\frac{\partial C}{\partial y} = Dm\frac{\partial^2 C}{\partial y^2} - k_r(C_w - C_\infty n)^n \tag{5}$$

The associated boundary conditions for Eqs. (1-5) are given by

$y = 0$: $u = U_w + A\frac{\partial u}{\partial y}$, $v = V_w(x)$, $N = -n\frac{\partial u}{\partial y}$, $T = Tw + B\frac{\partial T}{\partial y}$, C= Cw

$y \to \infty$: $u \to 0$, $N \to 0$, $T \to \infty$, $C \to \infty$. $\hspace{1cm}$ (6)

Here $u_w = U_0 e^{\frac{x}{L}}$ is the stretching velocity, $T_w = T_\infty + T_0 e^{\frac{2x}{L}}$ is the sheet temperature, U_0 is the reference velocity, T_0 is the reference temperature, $A = \alpha_1 e^{-\left(\frac{x}{2L}\right)}$ is the velocity slip factor which changes with x, $B = \beta_1 e^{-\left(\frac{x}{2L}\right)}$ is the thermal slip factor which changes with x (Mukhopadhyay [12]), the variable magnetic field is assumed to be $B(x) = B_0 e^{\left(\frac{x}{2L}\right)}$ (Seini and Makinde [17]), where B_0 is a constant magnetic field, positive and negative values of V_w indicates injection and suction respectively.

Also, u and v are velocity components in x and y directions respectively, $\rho, \kappa, T, C, N, \sigma, C_p, q_r, Q_0, k_r$ and n are fluid density, vortex viscosity, fluid temperature, fluid concentration, component of microrotation whose direction of rotation lies perpendicular to xy plane, electrical conductivity, specific heat at a constant pressure, radiative heat flux, heat source/sink, chemical reaction rate and order of chemical reaction. Similarly, A is the velocity slip, B is the thermal slip, k is the thermal conductivity, Dm is the molecular diffusivity, j is the spin gradient viscosity, and m is the microrotation boundary parameter with $0 \le m \le 1$. The case when $m = 0$ corresponds to $N = 0$ this represnts the no-spin condition i. e. strong concentration such that the particles close to the wall are unable to rotate. The case $m = \frac{1}{2}$ indicates weak concentration of micro-particles and the vanishing of anti-symmetric part of the stress tensor and the case $m = 1$ represents turbulent boundary layer flows (see Peddieson [35]; Ahmadi [36]; Jena and Mathur [37]).
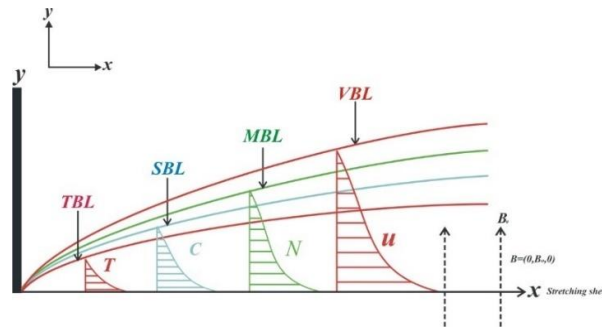

Fig. 1. Geometry of the flow

Using Rosseland approximation,

$$q_r = -\frac{4\sigma^*}{3\alpha^*}\frac{\partial T^4}{\partial y} \qquad (7)$$

is the radiative heat flux (Khedr et al. [38]; Akinbobola and Okoya [39]), here σ^* is Stefan-Boltzmann constant and α^* is the mean absorption coefficient.

Assuming that there exist sufficiently small temperature differences within the flow such that T^4 can be expressed as a linear combination of the temperature. Expanding T^4 in Taylor series about T_∞ to get

$$T^4 = T_\infty^4 + 4T_\infty^3(T - T_\infty) + +6T_\infty^2(T - T_\infty)^2 + \quad (8)$$

neglecting higher order terms in Eq. (8) gives

$$T^4 \approx 4T_\infty^3 T - 3T_\infty^4 \qquad (9)$$

hence

$$\frac{\partial q_r}{\partial y} = -\frac{16\sigma^* T_\infty^3}{3\alpha^*}\frac{\partial T^2}{\partial y} \qquad (10)$$

Following El-Aziz [15]; Seini and Makinde [17], the following similarity transformations are introduced

$$\eta = y\left(\frac{U_0}{2\nu L}\right)^{\frac{1}{2}}e^{\frac{x}{2L}}, \psi = (2\nu L U_0)^{\frac{1}{2}}e^{\frac{x}{2L}}f(\eta), u = \frac{U_0 e^x}{Lf'(\eta)}, T = T_\infty + T_0 e^{\left(\frac{x}{2L}\right)}\theta(\eta), \qquad (11)$$

$$v = \left(\frac{U_0}{2\nu L}\right)^{\frac{1}{2}}e^{\frac{x}{L}}(f(\eta) + \eta f'(\eta)), N = \left(\frac{U_0^3}{2\nu L}\right)^{\frac{1}{2}}e^{\frac{3x}{2L}}, \ C = C_\infty + C_0 e^{\left(\frac{x}{2L}\right)}\phi(\eta)$$

Where η is the dimensionless similarity variable, ψ is the stream function defined as $u = \frac{\partial\psi}{\partial y}, v = -\frac{\partial\psi}{\partial x}$ which identically satisfies the mass conservation Eq.(1). $f(\eta)$ is the dimensionless stream function, $\theta(\eta)$ is the dimensionless temperature, $\phi(\eta))$ is the dimensionless concentration and prime denotes differentiation with respect to η.

Substituting Eq. (11) into (2-5) and using Eq. (8) in (4) yields the following non-linear ODEs

$$(1 + K)f''' + ff'' - 2f'^2 + Kg' + Gr\theta - Mf' = 0 \qquad (12)$$

$$\lambda g'' + fg' - 3f'g - 2H(2g + f'') = 0 \qquad (13)$$

$$\left(1 + \frac{4}{3}R\right)\theta'' + PrEc(1 + K)f''^2 - Pr(f'\theta - f\theta') + PrEcMf'^2 + Pr\theta = 0. \qquad (14)$$

$$\phi'' - Sc(f'\phi - f\phi') + Sc\zeta\phi^n = 0. \qquad (15)$$

Subject to the boundary conditions

$$\eta = 0: f' = 1 + \alpha f'', f = fw, g = -mf'', \theta = 1 + \beta\theta', \phi = 1$$
$$\eta \to \infty: f' = 0, g \to 0, \theta \to 0, \phi \to 0 \qquad (16)$$

Here, prime denotes differentiation with respect to η, $K = \frac{\kappa}{\mu}$ is the material parameter, $\alpha = \alpha_1\sqrt{\frac{U_0}{2\nu L}}$ is the velocity slip parameter, $\alpha_1 = -Ae^{-\left(\frac{x}{2L}\right)}$ is the initial value of the velocity slip factor, $\beta_1\sqrt{\frac{U_0}{2\nu L}}$ is the thermal slip parameter, $\beta_1 = -Be^{-\left(\frac{x}{2L}\right)}$ is the initial value of the thermal slip factor [12], $fw = -V_0\left(\frac{2L}{U_0\nu}\right)^{\frac{1}{2}}$ is the suction/injection parameter ($fw > 0$ suction , $fw < 0$ injection and $fw = 0$ corresponds to an impermeable sheet, $V_w = V_0 e^{\left(\frac{x}{2L}\right)}$ $Pr = \frac{\mu C_p}{k}$ is the Prandtl number, $\lambda = \frac{\gamma}{\rho j}$ the microrotation density parameter, $Q = 2L/\rho C_p u_w$ is the heat generation/absorption parameter, $R = (4\sigma^* T_\infty^3)/\alpha^* k$ is the radiation parameter, $H = \frac{\kappa L}{\rho j U_0}$ is the vortex viscosity parameter, $M = 2L\sigma B_0^2/U_0\rho$ is the magnetic field parameter, $zeta = 2Lk_r(C_w - C_\infty)^{n-1}/U_0$ is the reaction rate parameter, n is the order of chemical reaction and $Ec = \frac{u_w}{C_p(T_w - T_\infty)}e^{\left(\frac{2x}{L}\right)}$ is the Eckert number,

2.1 Physical Quantities of Engineering Interest

The quantities of engineering interest are the non-dimensional skin friction, the Nusselt number (rate of heat transfer) and the wall couple stress coefficient. Following [15], these are respectively defined as

$$C_{fx} = \frac{1}{\rho u_w^2}[(\mu + \kappa) + \kappa N]_{y=0}, \quad Nu_x = \frac{L}{(T_w - T_\infty)}\left(-\frac{\partial T}{\partial \bar{y}}\right)_{y=0}$$

$$Sh_x = \frac{L}{(C_w - C_\infty)}\left(-\frac{\partial C}{\partial \bar{y}}\right)_{y=0}, \quad M_w = \left(\gamma\frac{\partial N}{\partial y}\right) \qquad (17)$$

In dimensionless form the skin friction, Nusselt number, Sherwood number and the wall couple stress coefficient correspondingly become

$$\frac{1}{\sqrt{2}}(Re_x)^{\frac{1}{2}}C_{fx} = \left(1 + (1 - mK)\right)f''(0), \ \sqrt{2}(Re_x)^{-\frac{1}{2}}Nu_x = -\theta'(0),$$

$$\sqrt{2}(Re_x)^{-\frac{1}{2}}Sh_x = -\phi^{'}(0), M_w = \gamma \frac{u_w^2}{2vL}g^{'}(0) \quad (18)$$

where $Re_x = \frac{u_w L}{v}$ is the local Reynolds number

3. NUMERICAL SOLUTION

The coupled nonlinear differential equations (12-15) together with the boundary conditions (16) is a Boundary value problem (BVP) which are solved using shooting method alongside fourth order Runge-Kutta method. The higher order equations (12-15) which are of third order in f, and second order in g, θ and ϕ are reduced into a system of nine simultaneous equations of first order for nine unknowns. To solve this system, one needs nine initial conditions while only five initial conditions are available. Thus, there are still four initial conditions that are needed which are not given in the problem, these are: $f^{''}(0)$, $g^{'}(0) \quad \theta^{'}(0) \ and \ \phi'(\eta)$. However, the values of $f^{'}, g, \theta$ and ϕ are known as $\eta \rightarrow \infty$. These four end conditions are used to produce the four unknown initial conditions (p_1, p_2, p_3, p_4) at $\eta = 0$ by applying the shooting technique. To estimate the value of η_∞ we start with some initial guess value and solve the BVPs equations (12-16) to get $f^{''}(0), g^{'}(0), \theta^{'}(0) \ and \ \phi'(0)$. The procedure is repeated until two successive values of $f^{''}(0), g^{'}(0), \theta^{'}(0) \ and \ \phi^{'}(0)$ differ only after desired significant digit signifying the limit of the boundary along η. The last value of η are chosen as appropriate for a particular set of governing parameters for the determination of the dimensionless velocity $f'(\eta)$, microrotation $g(\eta)$, temperature $\theta(\eta)$ and concentration $\phi(\eta)$ across the boundary layer. To reduce the higher order equations to a system of first order differential equations we let:

$$f_1 = f, f_2 = f^{'}, f_3 = f^{''}, f_4 = g, f_5 = g^{'}, f_6 = \theta, f_7 = \theta^{'}, f_8 = \phi, f_9 = \phi^{'} \quad (19)$$

$$f_3^{'} = \frac{2f_2^{'2} - f_1 f_3 - K f_5 + M f_2}{(1+K)} \quad (20)$$

$$f_5' = \frac{3f_2 f_4 + 2H(2f_4 + f_3) - f_1 f_5}{\lambda} \quad (21)$$

$$f_7^{'} = \frac{Pr(f_2 f_6 - f_1 f_7) - Ec(1+K)f_3^2 - EcM f_2 f_6 f_2^2 - Q f_6)}{\left(1 + \frac{4}{3}R\right)} \quad (22)$$

$$f_7^{'} = Sc\zeta f_8^n + Sc(f_2 f_8 - f_1 f_9) \quad (23)$$

The boundary conditions now become

$$f_1(0) = fw, f_2(0) = 1 + \alpha f_3, f_3(0) = p_1, f_4(0) = -n f_3(0), \ f_5(0) = p_2, f_6(0) = 1 + \beta f_7(0),$$

$$f_7(0) = p_3, \ f_8(0) = 1, \ f_9(0) = p_4, f_2(\infty) \rightarrow 0, f_4(\infty) \rightarrow 0, \ f_6(\infty) \rightarrow 0, f_8(\infty) \rightarrow 0 \quad (24)$$

After obtaining all the initial conditions, fourth-order Runge-Kutta integration scheme with step size $\nabla \eta = 0.05$ is applied and the solution is obtained with a tolerance limit of 10^{-7}. The skin friction cofficient $f^{''}(0)$, the local Nusselt number $-\theta^{'}(0)$, the sherwood number $-\phi'(0)$ and the wall couple stress $g^{'}(0)$ are found and presented in Table 3.

4. RESULTS AND DISCUSSION

To have clear insight into the behaviour of the fluid flow, a computational analysis has been carried out for the dimensionless velocity, temperature, concentration and microrotation for various values of the velocity slip parameter α, thermal slip parameter β, material (micropolar) parameter K, vortex viscosity parameter λ, radiation parameter R , chemical rate of reaction parameter ζ, order of chemical reaction parameter n , suction/injection parameter fw , heat generation parameter Q. The default values adopted for computation are: $K = \beta = \lambda = n = \zeta = M = 1, Pr = 0.72, R = Ec = 0.1, Q = -0.2, H = m = 0.5 \ and \ Sc = 0.62$. The graphs correspond to these values unless otherwise indicated.

In order to verify the accuracy of the numerical scheme used in this work, comparisons of the present results in respect to the values of the Nusselt number $-\theta'(0)$ have been made with the existing work of Bidin and Nazar [34], Ishak [35], Seini and Makinde [17] and Mukhopadhyay [12] in some limiting cases as shown in Table 1. The comparison is found to be in good agreement.

Table 2 depicts the values of the skin friction coefficient $f''(0)$ and the Nusselt number $-\theta'(0)$ (heat transfer rate) for variation in radiation parameter R, magnetic field parameter M and Eckert number Ec as compared with that of Seini and Makinde [17] in the absence of the velocity slip parameter α, thermal slip parameter β, material (micropolar) parameter K and suction/injection parameter fw. The comparison is found to be in good agreement.

Table 1. Values of $-\theta'(0)$ for variation in Pr and R compared to existing results when $\alpha = \beta = K = Sc = zeta = M = H = fw = \lambda = Q = Ec = n = 0$

Pr	R	Bidin & Nazar [40]	Ishak [41]	Seini & Makinde [17]	Mukhopadhyay [12]	Present
1.0	0.0	0.9547	0.9548	0.984811	0.9547	0.9548106
3.0		1.8691	1.8691	1.869060	1.8691	1.8690688
5.0			2.5001	2.500128	2.5001	2.5001280
10			3.6604	3.660369	3.6603	3.6603693
1.0	0.5	0.6765				0.6775462
1.0	1.0	0.5315	0.5312		0.5311	0.5353012
2.0	0.5	1.0735			1.0734	1.0735162
3.0		1.3807			1.3807	1.3807451

Table 2. Values of $f''(0)$ and $-\theta'(0)$ with [17] for variation in R, M and Ec when $Pr = 0.71, Sc = 0.24, \zeta = n = 1$ and $\alpha = \beta, K = H = m = 0$

			Seini & Makinde [17]		Present results	
R	M	Ec	$-f''(0)$	$-\theta'(0)$	$-f''(0)$	$-\theta'(0)$
0.0	1.0	1.0	1.629178	0.006338	1.629178	0.006338
0.1			1.629178	0.006964	1.629178	0.006965
0.5			1.629178	0.035754	1.629178	0.459923
0.1	2.0		1.912620	-0.276418	1.912620	-0.276418
	5.0		2.581130	-0.874464	2.581130	-0.874464
	10.0		3.415289	-1.153452	3.415290	-1.153452
	1.0		1.629178	-0.006964	1.629178	-0.006965
		2.0	1.629178	-0.598521`	1.629178	-0.598521`
		3.0	1.629178	-1.204006	1.629178	-1.204006

Table 3 displays the computational values of the skin friction coefficient, the local Nusselt number, the local Sherwood number and the wall couple stress coefficient for variation in the velocity slip parameter α. thermal slip parameter β material parameter K, heat source/sink parameter Q, suction/injection parameter and chemical reaction parameter ζ. From this table, it is found that an increase in the velocity slip parameter α causes a reduction in the skin friction, Nusselt number, Sherwood number and the wall couple stress coefficient whereas an increase in fw has the exact opposite effect. Similarly, a rise in the thermal slip parameter β decreases the Nusselt number while it has no effect on the skin friction coefficient, Sherwood number and the wall couple stress coefficient. A rise in the material parameter K leads to a decrease in both the skin friction and the wall couple stress coefficient while the opposite trend is observed for the heat and mass transfer rates. The rate of mass transfer also increases with an increase in the rate of chemical reaction ζ.

Figs. 2-3 depict the influence of magnetic field parameter M on the velocity and temperature profiles. Evidently, the velocity decreases with an increase in the value of the magnetic field parameter M. This response is due to the imposition of the transverse magnetic field in an electrically conducting fluid which induces a drag-like force known as Lorentz force which act against the fluid motion and slows it down. However, the temperature rises with increasing values of M as displayed in Fig. 3.

Figs. 4-7 illustrate the influence of the material parameter K on the velocity, temperature, microrotation and concentration profiles. It is evident that the velocity profile increases with an increase in K due to the increase in the hydrodynamic boundary layer thickness as shown in Fig. 4. On the other hand, the temperature, concentration and the microrotation profiles decrease as K increases. The decrease in the microrotation profiles however, is only near the stretching sheet, further from the sheet, the profile overlap and then increase as displayed in Fig. 6.

Table 3. Values of $-f''(0), -\theta''(0), \phi'(0)$ and $g'(0)$ for varying values of α, β, K, Q, fw and ζ

α	β	K	Q	Fw	ζ	$-f''(0)$	$-\theta'(0))$	$-\phi'(0))$	$g'(0)$
0.0	1.0	1.0	-0.2	0.5	1.0	1.165924	0.466564	0.498763	1.025623
0.5						0.681269	0.454178	0.432430	0.496035
1.5						0.387813	0.432699	0.378757	0.233498
0.3	1.0					0.811615	0.888203	0.452322	0.628176
	2.0					0.811615	0.605753	0.452322	0.628176
	3.0					0.811615	0.370265	0.452322	0.628176
	1.0	0.0				1.130453	0.434659	0.891765	0.873466
		1.0				0.811615	0.459601	0.994994	0.628176
		2.0				0.664698	0.469187	1.047335	0.513730
		1.0	0.05			0.811615	0.417220	1.096904	0.628176
			0.15			0.811615	0.391803	1.096904	0.628176
			0.5			0.811615	0.311219	0.672770	0.325540
				-1.0		0.688525	0.356113	0.789315	0.401561
				-0.5		0.811615	0.459600	1.096904	0.628176
				0.5		0.881867	0.510266	1.286923	0.792278
				1.0	0.2	0.811615	0.459600	0.584242	0.628176
				0.5	1.0	0.811615	0.459600	0.758253	0.628176
					0.5	0.811615	0.459600	0.883001	0.628176
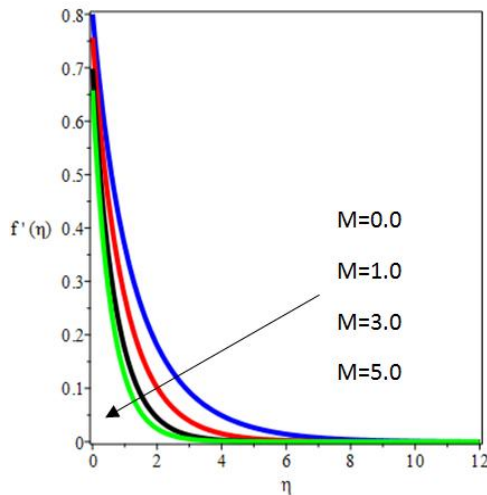
Fig. 2. Effect of *M* on velocity profiles
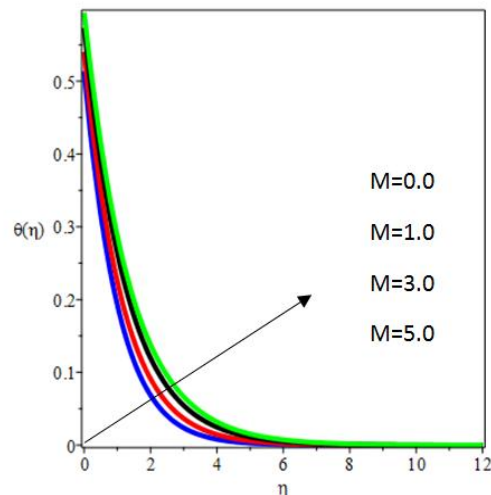
Fig. 3. Effect of *M* on temperature profiles

Figs. 8-9 describe the effects of the velocity slip parameter α on the velocity and temperature profiles across the boundary layer. There is a reduction in the fluid velocity as α increases as shown in Fig. 8. Moreover, it is noticed that the rate of transport reduces with the increasing distance η from the sheet for the velocity profiles. In the presence of slip, the stretching velocity and the flow velocity near the sheet are unequal. Therefore, an increase in the slip parameter α causes a rise in the slip velocity leading to a decrease in the fluid velocity as observed in Fig. 8. Meanwhile, an increase in α enhances the temperature distribution due to the thickening of

the thermal boundary layer thickness as shown in Fig. 9. Fig. 10 shows that an increase in the thermal slip parameter β causes a decrease in temperature profiles. This response is due to the fact that as β increases, less heat is transferred from the sheet to the fluid leading to a drop in the temperature (see Table 3).

Figs. 11-13 describe the influence of the suction/injection parameter fw on the velocity, temperature and concentration profiles. A decrease in the velocity, temperature and microrotation profiles is observed with an increase in the suction parameter $fw > 0$. An

increase in $fw > 0$ causes thinning effects on these profiles due to the fact that the heated fluid is being pushed towards the sheet such that the fluid is brought closer to the surface leading reduction in the, momentum, thermal and solutal boundary layer thicknesses. However, the imposition of wall fluid injection $fw < 0$ produces the opposite effect as it enhances velocity, thermal and solutal distribution within the boundary layer. Fig. 14 describes the variation of temperature profiles with η for different values of Eckert number Ec . Observation shows that increasing values of Ec enhances temperature distribution and the thermal boundary layer thickness. This response is due the fact that as Ec increases, heat is generated as a result of the

drag between the fluid particles, the internal heat generation inside the fluid increases the bulk fluid temperature which is an indication of additional heating in the flow region due to viscous dissipation, thus, the additional heat causes increase in the fluid temperature. The effect of radiation parameter R on the temperature distribution is displayed in Fig. 15. Evidently, the temperature profile increases as the magnitude of R increases. This is due to the fact that the divergence of the radiative heat flux increases as the Rosseland mean absorption coefficient decreases. Thus, the rate of radiative heat transfer to the fluid rises and then causing the temperature of the fluid to rise. Hence, the cooling process is at a faster rate if R reduced.
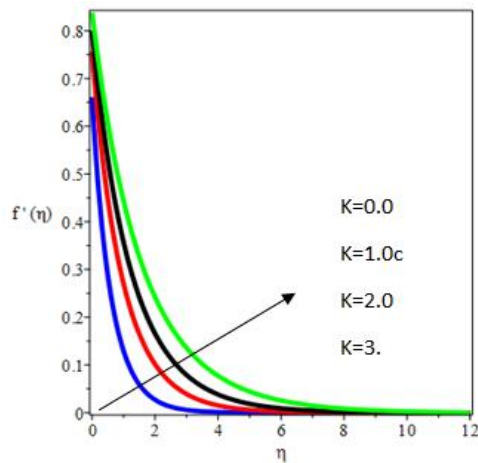
Fig. 4. Effect of *K* on velocity profiles
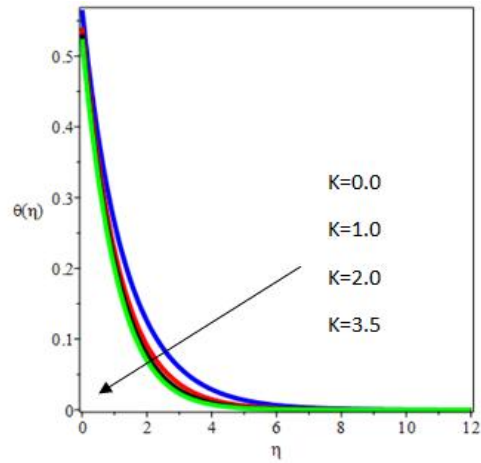
Fig. 5. Effect of *K* on temperature
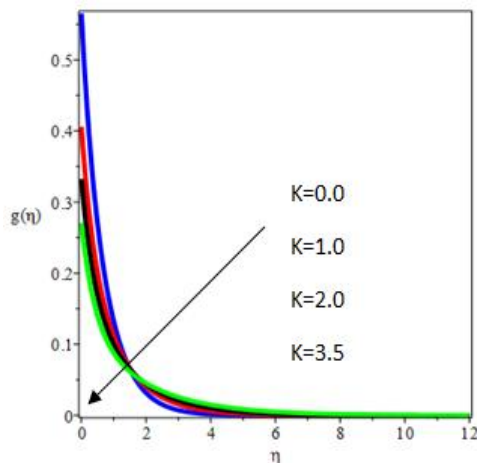
Fig. 6. Effect of *K* on microrotation profiles
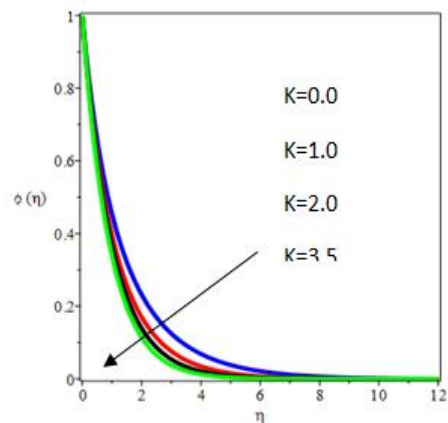
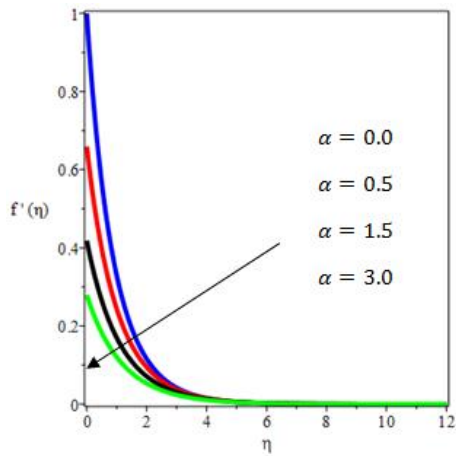**Fig. 7. Effect of *K* on concentration profiles**

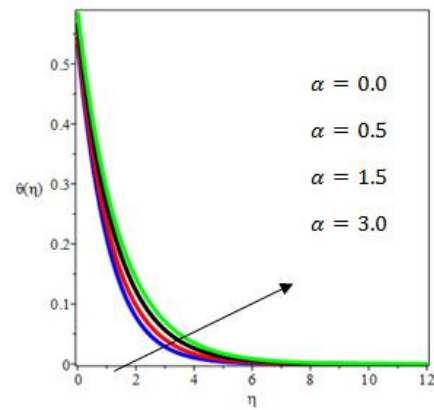**Fig. 8. Effect of α on velocity profiles**

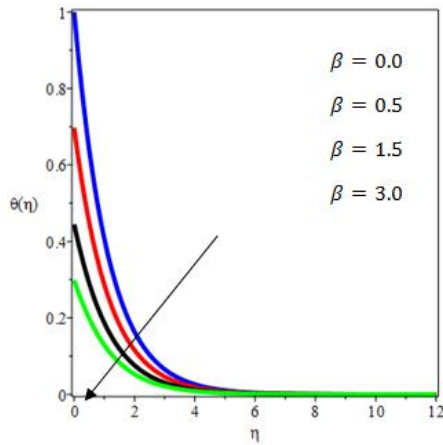**Fig. 9. Effect of α on temperature profiles**
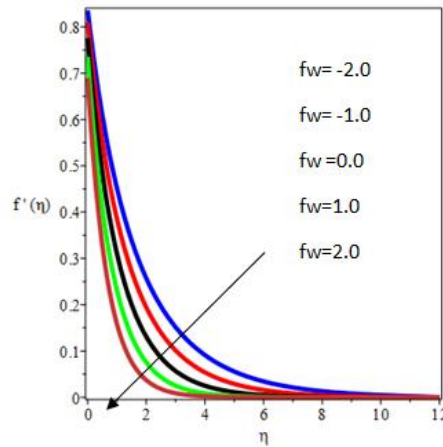

Fig. 10. Effect of β on temperature profiles
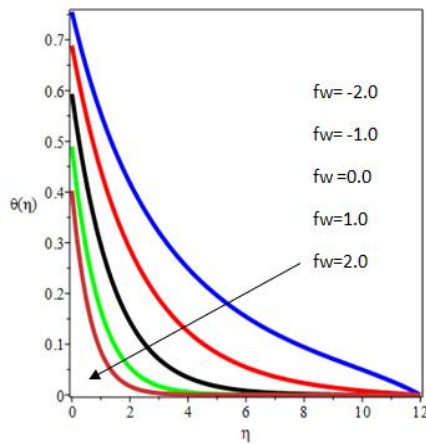

Fig. 11. Effect of fw on velocity profiles

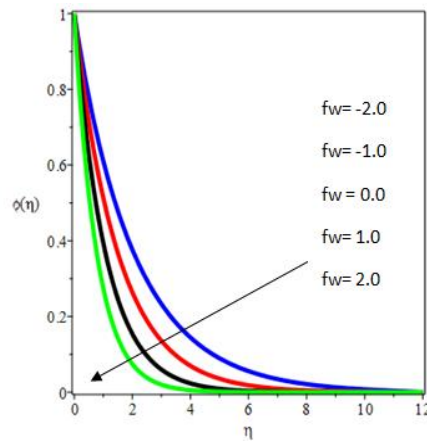**Fig. 12. Effect of fw on temperature profiles**

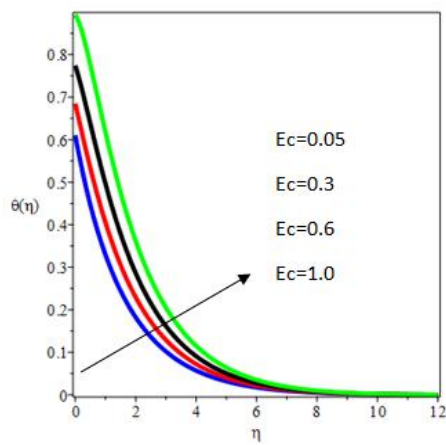**Fig. 13. Effect of fw on concentration profiles**

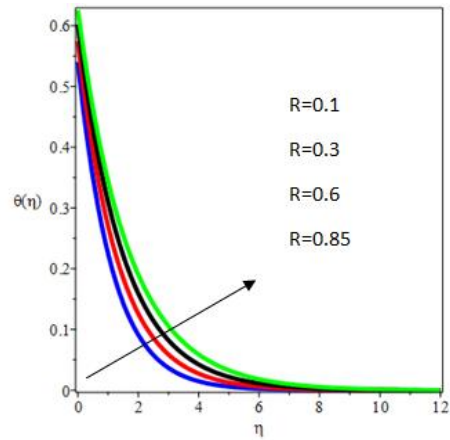**Fig. 14. Effect of Ec on temperature profiles**

Fig. 15. Effect of R on temperature
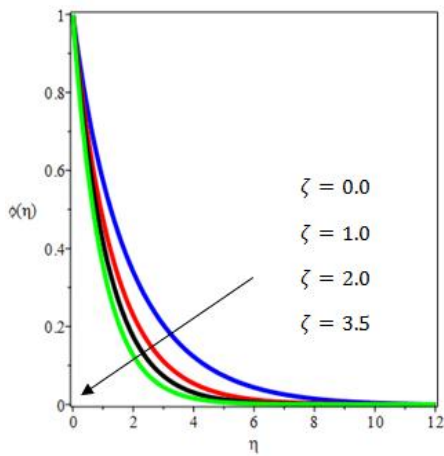

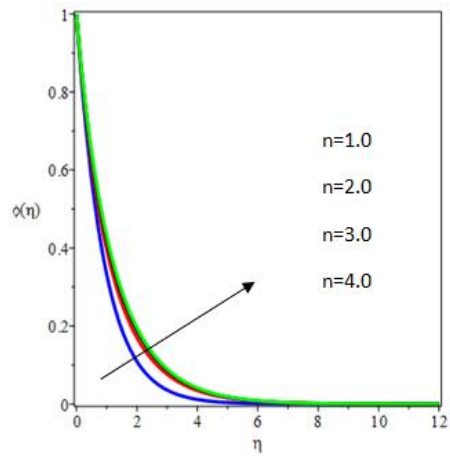**Fig. 16. Effect of ζ on concentration profiles**

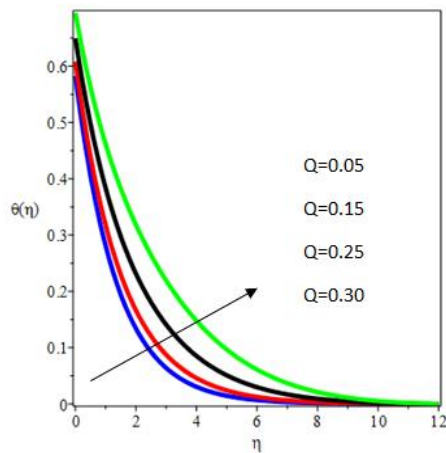**Fig. 17. Effect of n on concentration profiles**

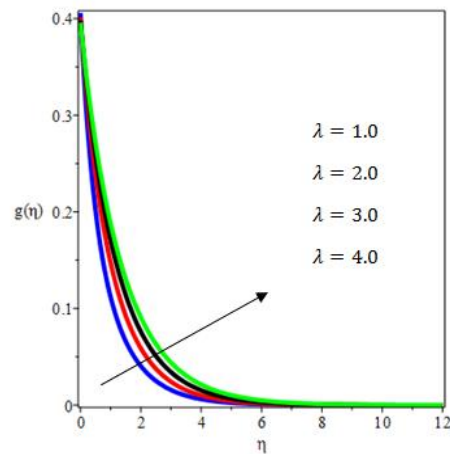**Fig. 18. Effect of Q on temperature profiles**

Fig. 19. Effect of λ on microrotation

Fig. 16 depicts the influence of the homogeneous chemical reaction rate parameter ζ on the concentration profiles. An increase in ζ causes a decrease in the concentration of the micropolar fluid flow along the exponentially stretching sheet due to the thinning of the solutal boundary layer thickness. In contrast, an increase in the order of the chemical reaction n enhances the concentration profiles as shown in Fig. 17.

The influence of heat generation parameter Q on the dimensionless temperature profile is illustrated in Fig. 18. Clearly, an increase in Q enhances the temperature distribution due to a rise in the thermal boundary layer thickness as Q increases. In addition, energy is generated by the imposition $Q > 0$ leading to an increase in the micropolar fluid temperature, thereby causing a rise in the temperature profiles. Fig. 19 describes the effect of the microrotation density parameter λ on the microrotation profiles. It is noticed that the microrotation profile rises with an increase in λ due to a rise in the microrotation boundary layer thickness.

5. CONCLUSION

The problem of hydromagnetic micropolar fluid flow, heat and mass transfer over an exponentially stretching sheet under the influence of thermal radiation, viscous dissipation, surface mass flux, chemical reaction and slip effects has been investigated. The resulting equations governing the fluid flow are solved using shooting method alongside Runge-Kutta integration technique. The results compared well with the existing results in the literature in some limiting cases. The influences of the emerging physical parameters on the dimensionless velocity, microrotation, temperature and species concentration profiles as well as on the skin friction coefficient $f''(0)$, wall couple stress coefficient $g'(0)$, Nusselt number $-\theta'(0)$ and the Sherwood number $\phi'(0)$ are presented through graphs and tables. The following conclusions are drawn from this study:

- The material (micropolar) parameter K causes a reduction in the skin friction coefficient $f''(0)$ and the wall couple stress $g'(0)$ whereas the rate of heat transfer $-\theta'(0)$ and mass transfer $-\phi'(0)$ rise with an increase in K. Thus, the material parameter K can be useful in reducing drag along the stretching sheet while it increases the rate of heat transfer.

- An increase in the velocity slip parameter α also reduces the skin friction coefficient $f''(0)$ as the thermal slip parameter β reduces the rate of heat transfer.
- An increase in the order of the chemical reaction enhances the concentration profiles as the rate of mass transfer is enhanced by the chemical reaction rate. However, the rate of the chemical reaction causes a decrease in the species concentration of the micropolar fluid flow.

The thermal radiation, heat generation as well as viscous dissipation enhances the temperature profiles and the thermal boundary layer thickness while the trend is reversed with the imposition of suction parameter.

COMPETING INTERESTS

Authors have declared that no competing interests exist.

REFERENCES

1. Eringen AC. Theory of micropolar fluids. J. Math. Anal. Appl. 1966;16:1-18.
2. Eringen AC. Theory of thermo-microfluids. Journal of Mathematical Analysis and Applications. 1972;38:480-496.
3. Chen J, Liang C, Lee JD. Theory and simulation of micropolar fluid dynamics. J. Nanoengineering and Nanosystems. 2011; 224:31-39.
4. Hayat T, Shehzad SA, Qasim M. Mixed convection flow of a micropolar fluid with radiation and chemical reaction. Int J. Numer Meth. 2011;67:1418-1436.
5. Lukaszewicz G. Micropolar fluids: Theory and Applications 1st Ed., Birkhauser, Boston; 1999.
6. Peddieson J, McNitt RP. Boundary layer theory for micropolar fluid, Recent Adv. Enggng Sci. 1970;5:405.
7. Crane LJ. Flow past a stretching plate, Communicatios Breves. 1970;21:645-647.
8. Gupta PS, Gupta AS. Heat and mass transfer on a stretching sheet with suction or blowing, Can. J. Chem. Eng. 1977;55: 744-746.
9. Eldabe NT, Elshehawey EF, Elbarbary ME. Elgazery NS. Chebyshev finite difference method for MHD flow of a micropolar fluid past a stretching sheet with heat transfer, Journal of Applied Mathematics and Computation. 2003;160:437-450.

10. Elbashbeshy EMA, Bazid MAA. Heat transfer in a porous medium over a stretching surface with internal heat generation and suction or injection. Applied Mathematics and Computation. 2004;158: 799-807.

11. Reddy MG. Heat generation and thermal radiation effects over a stretching sheet in a micro polar fluid. Int. Scholarly Research Network. 2012;2012:1-6.

12. Mukhopadhyay S. Slip effects on MHD boundary layer flow over an exponentially stretching sheet with suction/blowing and thermal radiation, Ain Shams Engineering Journal. 2013;2013:485-491.

13. Magyari E, Keller B. Heat and mass transfer in the boundary layers on an exponentially stretching continuous surface. Journal of Physics. 1999;32577-585.

14. Sajid, M, Hayat T. Influence of thermal radiation on thermal radiation on the boundary layer flow due to exponentially stretching sheet. International Communication in Heat and Mass Transfer. 2008;35:347-356.

15. El-Aziz M. Viscous dissipation effect on mixed convection flow of a micropolar fluid over an exponentially stretching sheet. Can. J. Phy. 2009;87:359-368.

16. Mandal, I. and Mukhopadhyay, S. Heat transfer analysis for fluid flow over an exponentially stretching porous sheet with surface heat flux. Ain Shams Eng. Journal. 2013; 2013, 103-110.

17. Seini YI, Makinde OD. MHD boundary layer flow due to exponentially stretching surface with radiation and chemical reaction. Mathematical Problem in Engineering. 2013;2013:1-7.

18. Daniel YS. Steady MHD boundary-layer slip flow and heat transfer of Nanofluid over a convectively heated of a non-linear permeable sheet. Journal of Advanced Mechanical Engineering. 2016;3:1-14.

19. Kumar L. Finite element analysis of combined heat and mass transfer in hydromagnetic micro polar flow along a stretching sheet. Comput Mater Sci. 2009; 46:841-848.

20. Daniel YS, Aziz ZA, Ismail Z, Salah F. Impact of thermal-radiation on electrical MHD flow of nanofluid over nonlinear stretching sheet with variable thickness. Alexandria Engineering Journal. 2017; 1-11.

21. Daniel YS, Aziz ZA, Ismail Z, Salah F. Thermal radiation on unsteady electrical MHD flow of nanofluid over stretching sheet with chemical reaction. Journal of King Saud University Science. 2017;1-9. Available:doi.org/10.1016/j.jksus.2017.10.002.

22. Biswas R, Mondal M, Sarkar DR, Ahmed SF. Effects of thermal radiation and chemical reaction on MHD unsteady heat and mass transfer of Casson fluid flow past a vertical plate. Journal of Advances in Mathematics and Computer Science. 2017;32:1-16.

23. Daniel YS, Daniel SK. Effects of buoyancy and thermal radiation on MHD flow over a stretching porous sheet using homotopy analysis method, Alexandra Engineering Journal. 2015;1-8. Available:http://dx.doi.org/10.1016/j.aej.2015.03.029

24. Das K. Slip effects on heat and mass transfer in MHD micropolar fluid flow over an inclined plate with thermal radiation and chemical reaction. Int. J. Numer. Meth. Fluids; 2012. DOI: 10.2002/fd.2683

25. Mishra SR, Baag S, Mohapatra hydro magnetic micropolar fluid along DK. Chemical reaction and Soret effects on a stretching sheet. Engineering Science and Technology, an International Journal. 2016;19:1919-1928.

26. Ibrahim SM. Effects of chemical reaction on dissipative radiative MHD flow through a porous medium over a nonisothermal stretching sheet, Journal of Industrial Mathematics, Research. 2014;1-10(2010).

27. Olajuwon BI, Oahimire JI, Waheed WA. Convection heat and mass transfer in a hydro magnetic flow of a micropolar fluid over a porous medium. Theoret. Appl. Mech. 2014;41:93-117.

28. Fatunmbi EO, Odesola AS. MHD free convective heat and mass transfer of a micropolar fluid flow over a stretching permeable sheet with constant heat and mass flux. Asian Research Journal of Mathematics. 2018;9:1-18.

29. Pal D, Chatterjee S. Heat and mass transfer in MHD non-Darcian flow of a micropolar fluid over a stretching sheet embedded in a porous media with non-uniform heat source and thermal radiation,

Available:doi.org/10.1016/j.acj.2017.07.007

Commun Nonlinear Sci. Numer Simulat. 2011;15:1843-1857.

30. Wang CY. Flow due to stretching boundary with partial slip- an exact solution of the Navier Stokes equation. Chen Eng. Sci. 2002;57:3745-3747.

31. Anderson HI. Sip flow past a stretching surface. Acta Mechanica. 2002;158:121-125.

32. Daniel YS. Laminar convective boundary layer slip flow over a flat plate using homotopy analysis method. J. Inst. Eng. India. Ser. E. 2016;1-7.
DOI: 10.1007/s40034-016-0084-6

33. Devi RL, Neeraja A, Reddy NB. Radiation effect on MHD slip flow past a stretching sheet with variable viscosity and heat source/sink. Int. J. Sci and Innovative Mathematical Res. 2015;3:8-17.

34. Nandeppanavar MM, Vajravelu K, Abel MS, Siddalingappa MN. MHD flow and heat transfer over a stretching surface with variable thermal conductivity and partial slip. Meccanica. 2013;48:1451-1464.

35. Peddieson J. An application of the micropolar model to the calculation of a turbulent shear flow. Int. J. Eng. Sci. 1972; 10:23-32.

36. Ahmadi G. Self-similar solution of incompressible micropolar boundary layer flow over a semi-infinite plate. Int. J. Engng Sci. 1976;14:639-646.

37. Jena SK, Mathur MN. Similarity solutions for laminar free convection flow of a thermo micropolar fluid past a non-isothermal flat plate. International J. Eng. Sci. 1981;19:1431-1439.

38. Khedr MEM, Chamkha AJ, Bayomi M. MHD flow of micropolar fluid past a stretched permeable surface with heat generation or absorption, Nonlinear Analysis Modelling. 2009;14:27-40.

39. Akinbobola TE, Okoya SS. The flow of second grade fluid over a stretching sheet with variable thermal conductivity and viscosity in the presence of heat source/sink. Journal of Nigeria Mathematical Society. 2015;34:331-342.

40. Bidin B, Nazar R. Numerical solution of the boundary layer over an exponentially stretching sheet. European Journal of Scientific Research. 2009;33:710-717.

41. Ishak A. MHD boundary layer flow due to exponentially stretching sheet with radiation effect. Sains Malayansian. 2011; 40:391-395.